Progress In Electromagnetics Research B, Vol. 15, 57–76, 2009

FIELD AROUND THE FOCAL REGION OF A PARABOLOIDAL REFLECTOR PLACED IN ISOTROPIC CHIRAL MEDIUM

T. Rahim and M. J. Mughal

Faculty of Electronic Engineering
GIK Institute of Engineering Sciences and Technology
Topi, Swabi 23640, N.W.F.P., Pakistan

Q. A. Naqvi and M. Faryad

Electronics Department
Quaid-i-Azam University
Islamabad 45320, Pakistan

Abstract—High frequency field expressions are derived at the focal points of a paraboloidal reflector placed in a homogenous and reciprocal chiral medium. Firstly Geometrical Optics (GO) field expressions are derived for the paraboloidal reflector placed in chiral medium. As the GO fails at the focal points, so Maslov's method has been used to find the field expressions which are also valid around the focal point. By using hybrid space, Maslov's method combine the simplicity of ray theory and the generality of Fourier Transform method. Some numerical results including contour plots and line plots around the focal region of paraboloidal reflector placed in chiral medium are obtained using the derived expressions.

1. INTRODUCTION

Asymptotic ray theory (ART) or the geometrical optics approximation is widely used to study various kinds of problems in the areas of electromagnetic, acoustic waves, seismic waves etc [1–3]. As geometrical optics (GO) fails in the focal regions, so Maslov's method is used to study the fields at the focal regions [4, 5]. Maslov's method combines the simplicity of asymptotic ray theory and the generality of the Fourier transform method. This is achieved by representing

Corresponding author: T. Rahim (rahim372@gmail.com).

the geometrical optics fields in hybrid coordinates consisting of space coordinates, and wave vector coordinates, that is by representing the field in terms of six coordinates. It may be noted that information of ray trajectories is included in both space coordinates $\mathbf{R} = (x, y, z)$ and wave vector coordinates $\mathbf{P} = (p_x, p_y, p_z)$. Solving the Hamiltonian equations under the prescribed initial conditions, one can construct the geometrical optics field in space $\mathbf{R}$, which is valid except in the vicinity of focal point. Near the focal point, the expression for the geometrical optics field in spatial coordinates is rewritten in hybrid domain. The expression in hybrid domain is related to the original domain $\mathbf{R}$ through the asymptotic Fourier transform. The reason for considering the hybrid domain is that, in general the singularities in different domain do not coincides. This means that a domain always exist in which the solution is bounded. Analysis of focusing systems has been worked out by various authors using Maslov's method [6–20]. In present work, our interest is to apply the Maslov's method to a paraboloidal reflector placed in chiral medium. Chiral medium is microscopically continuous medium composed of chiral objects, uniformly distributed and randomly oriented [22]. A chiral object is a three dimensional body that can not be brought into congruence with its mirror image through translation or rotation e.g., helix, animal hands etc. An object which is not chiral is called achiral. A chiral medium is either right handed or left handed. The historical background and electromagnetic chirality has been analyzed by various authors [22–30].

2. GEOMETRICAL OPTICS AND MASLOV'S METHOD IN ORDINARY MEDIUM

The GO and Maslov's method is given in [6, 14], but here it is applied to a paraboloidal reflector placed in chiral medium, so first it is discussed for three dimensional wave in ordinary medium. Consider the scalar wave equation

$$\left(\nabla^2 + n^2k^2\right) u(r) = 0 \tag{1}$$

where $r = (x, y, z)$, $\nabla^2 = \partial^2/\partial_x^2 + \partial^2/\partial_y^2 + \partial^2/\partial_z^2$, $k = \omega\sqrt{\epsilon\mu}$ is wave number and n is index of refraction of the medium, which is constant in this case. Medium is homogeneous and isotropic. Solution of Eq. (1) may be assumed in the form of Luneberg-Kline series

$$u(r) = \sum_{m=0}^{\infty} \frac{E^m(r)}{(jk)^m} \exp(-jks) \tag{2}$$

Assuming large values of k, hence higher order terms are neglected, and only first term of Eq. (2), is taken. By putting Eq. (2) in Eq. (1) and equating the coefficient of k^2 we get Eikonal equation as in [21]

$$\{\nabla s(r)\}^2 - n^2 = 0 \tag{3}$$

similarly by equating the coefficients of k we get transport equation

$$2\nabla E \cdot \nabla s + E\nabla^2 s = 0 \tag{4}$$

where only E^0 is retained and is denoted by E. Wave vector and Hamiltonian are define as $\mathbf{p} = \nabla s$ and $H(r, p) = (\mathbf{p} \cdot \mathbf{p} - n^2)/2$ respectively. So the Eikonal equation becomes $H(r, p) = 0$. Eikonal equation can be solved by the method of characteristic as follow

$$\frac{dx}{dt} = p_x \tag{5}$$

$$\frac{dy}{dt} = p_y \tag{6}$$

$$\frac{dz}{dt} = p_z \tag{7}$$

$$\frac{dp_x}{dt} = 0 \tag{8}$$

$$\frac{dp_y}{dt} = 0 \tag{9}$$

$$\frac{dp_z}{dt} = 0 \tag{10}$$

The solution of Eqs. (5)–(10) are

$$x = \xi + p_x t \tag{11}$$

$$y = \eta + p_y t \tag{12}$$

$$z = \zeta + p_z t \tag{13}$$

$$p_x = p_{x_0} \tag{14}$$

$$p_y = p_{y_0} \tag{15}$$

$$p_z = p_{z_0} \tag{16}$$

where, (ξ, η, ζ) and (p_{x0}, p_{y0}, p_{z0}) are the initial values of (x, y, z) and (p_x, p_y, p_z) respectively. The phase function is given by

$$s = s_0 + \int_0^t n^2 dt = s_0 + n^2 t \tag{17}$$

Applying Gauss's theorem to a paraxial ray tube, we obtain the solution of Eq. (4) as in [21]

$$u(r) = Er_0 J^{-1/2} \exp\left\{-jk\left(s_0 + n^2 t\right)\right\} \tag{18}$$

where Er_0 is the initial value of the field amplitude and $J = D(t)/D(0)$, where $D(t) = \partial(x, y, z)/\partial(\xi, \eta, \zeta)$, is the Jacobian of transformation from ray coordinates (ξ, η, ζ) to cartesian coordinate (x, y, z). The GO solution is not valid at focal points that is where $J = 0$, so Maslov's method is used to find the fields around the focal regions of a focusing system as in [6–21]. The equation which is valid around the focal point of a paraboloidal reflector placed in ordinary medium is given as [6]

$$\begin{aligned} u(r) \;=\; & \frac{k}{2\pi}\int_{-\infty}^{\infty}\int_{-\infty}^{\infty} E_{r0}\left(\frac{D(t)}{D(0)}\frac{\partial(p_x, p_y)}{\partial(x, y)}\right)^{-\frac{1}{2}} \exp[-jk\{s_0 + n^2 t \\ & -x(p_x, p_y, z)p_x - y(p_x, p_y, z)p_y + xp_x + yp_y\}]dp_x dp_y \end{aligned} \tag{19}$$

The expression $\frac{D(t)}{D(0)}\frac{\partial(p_x,p_y)}{\partial(x,y)}$ can be more simply calculated as

$$\frac{D(t)}{D(0)}\frac{\partial(p_x, p_y)}{\partial(x, y)} = \frac{1}{D(0)}\frac{\partial(p_x, p_y, z)}{\partial(\xi, \eta, \zeta)} \tag{20}$$

3. GEOMETRICAL OPTICS IN CHIRAL MEDIUM

Both left circularly polarized (LCP) and right circularly polarized (RCP) modes, are supported by chiral medium. There are many ways to define the constitutive relations for chiral medium, but Drude-Born-Fadorov (DBF) constitutive relations [22] are used as follows

$$\mathbf{D} = \epsilon(\mathbf{E} + \beta\nabla \times \mathbf{E}) \tag{21}$$

$$\mathbf{B} = \mu(\mathbf{H} + \beta\nabla \times \mathbf{H}) \tag{22}$$

where, ϵ, μ, and β is permittivity, permeability and chirality parameters respectively, ϵ, μ, have usual dimensions and β has the dimension of length. Using Eq. (21) and Eq. (22), solution of Maxwell's equations results in coupled differential equations. Uncoupled differential equations for $\mathbf{E}$ and $\mathbf{H}$ are obtained by using the following transformation [22]

$$\mathbf{E} = \mathbf{Q}_L - j\sqrt{\frac{\mu}{\epsilon}}\mathbf{Q}_R \tag{23}$$

$$\mathbf{H} = \mathbf{Q}_R - j\sqrt{\frac{\epsilon}{\mu}}\mathbf{Q}_L \tag{24}$$

and $\mathbf{Q}_L$, $\mathbf{Q}_R$ are RCP and LCP wave respectively and satisfy the following equations

$$\left(\nabla^2 + n_1^2 k^2\right) \mathbf{Q}_L = 0 \tag{25}$$

$$\left(\nabla^2 + n_2^2 k^2\right) \mathbf{Q}_R = 0 \tag{26}$$

where, $n_1 = 1/(1 - k\beta)$ and $n_2 = 1/(1 + k\beta)$ are equivalent refractive indices for LCP and RCP waves respectively and $k = \omega\sqrt{\epsilon\mu}$. The Eq. (25) and Eq. (26) show that fields in chiral medium may be treated in a manner similar to ordinary medium if the transformation given in Eq. (23) and Eq. (24) are used. So GO solution for chiral medium can be obtained in a manner similar to ordinary medium as discussed. Now in chiral medium two types of polarizations exist, so both waves are solved independently. The total field will be the superposition of the two contributions.

4. GEOMETRIC OPTICS FIELD OF A PARABOLOIDAL REFLECTOR PLACED IN CHIRAL MEDIUM

In this paper, we want to find the reflected field around the focal region of a paraboloidal reflector placed in a chiral medium. To achieve this the reflection of plane waves from simple perfect electric conducting (PEC) plane placed in chiral medium is discussed as in [14]. Reflection of RCP wave with unit amplitude, phase velocity ω/kn_2 and making angle α with z-axis, from a perfect electric conducting (PEC) plane has been considered in Figure 1. Two waves are reflected, a RCP wave with amplitude $(\cos\alpha - \cos\alpha_1)/(\cos\alpha + \cos\alpha_1)$, traveling with phase velocity ω/kn_2 and making an angle α with z-axis and an LCP wave with amplitude $2\cos\alpha/(\cos\alpha + \cos\alpha_1)$ traveling with phase velocity ω/kn_1 and making an angle $\alpha_1 = \sin^{-1}\{(n_1/n_2)\sin\alpha\}$ with z-axis. If we take $\beta > 0$ then $n_1 > n_2$ and $\alpha_1 < \alpha$, LCP wave bends towards normal, because it is slower than RCP. In Figure 2, LCP wave with

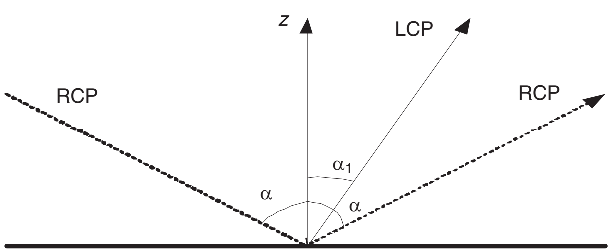

Figure 1. RCP reflection from PEC plane.

unit amplitude, and angle α with z-axis, is incident on perfect electric conducting (PEC) plane we get two reflected waves, a RCP wave with amplitude $2\cos\alpha/(\cos\alpha+\cos\alpha_2)$ traveling with phase velocity ω/kn_2 and making an angle $\alpha_2 = \sin^{-1}\{(n_2/n_1)\sin\alpha\}$ with z-axis and an LCP wave with amplitude $(\cos\alpha - \cos\alpha_2)/(\cos\alpha+\cos\alpha_2)$ traveling with phase velocity ω/kn_1 and making an angle α with z-axis. If we take $\beta > 0$ then $n_1 > n_2$ and $\alpha_2 > \alpha$. If $\beta = 0$ then only normal reflection take place, and if β increases the difference between the angle α and α_1, α_2 increases.

Four waves are reflected when both LCP and RCP waves hit the PEC plane. These waves are represented by RR, RL, LL and LR, where RR and RL are RCP and LCP reflected wave components respectively, when RCP is incident, and LL and LR are LCP and RCP reflected waves respectively, when incident wave is LCP. Consider a paraboloidal reflector, as shown in Figure 3, having Equation given as

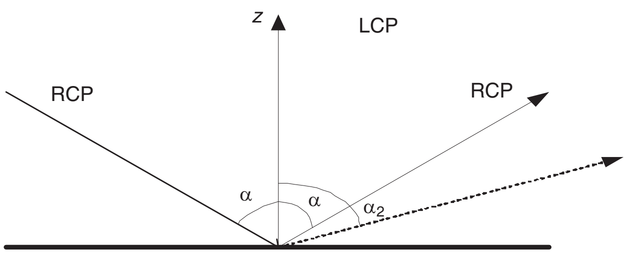

Figure 2. LCP reflection from PEC plane.

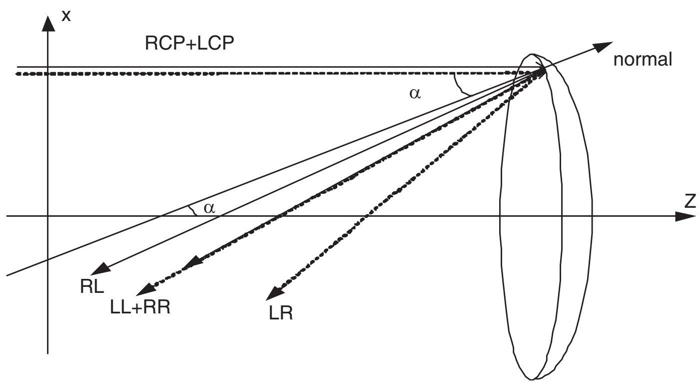

Figure 3. Paraboloidal reflector placed in chiral medium.

$$\zeta = g(\xi, \eta) = f - \frac{\rho^2}{4f} = f - \frac{\xi^2 + \eta^2}{4f} \tag{27}$$

where, (ξ, η, ζ) are the initial values of (x, y, z), f is the focal length of the paraboloidal reflector and $\rho^2 = \xi^2 + \eta^2$. The reflector is placed in homogenous and reciprocal chiral medium defined by constitutive relations as given in Eq. (21) and Eq. (22). Let there be two incident plane waves of opposite handedness traveling in chiral medium along positive z-axis, which satisfy the wave equations (25) and (26) are given as

$$\mathbf{Q}_L = (\mathbf{a}_x + j\mathbf{a}_y) \exp(-jkn_1 z) \tag{28}$$

$$\mathbf{Q}_R = (\mathbf{a}_x - j\mathbf{a}_y) \exp(-jkn_2 z) \tag{29}$$

where $\mathbf{a}_x$ and $\mathbf{a}_y$ are the unit vector along x-axis and y-axis respectively. By ignoring the polarization and taking the incident field of unit amplitude we get

$$Q_L = \exp(-jkn_1 z) \tag{30}$$

$$Q_R = \exp(-jkn_2 z) \tag{31}$$

These waves are making an angle α with the normal to the surface of a paraboloidal reflector. The unit normal vector to the surface can be written as

$$\mathbf{a}_n = \sin\alpha \cos\gamma \mathbf{a}_x + \sin\alpha \sin\gamma \mathbf{a}_y + \cos\alpha \mathbf{a}_z \tag{32}$$

where, α and γ are given as

$$\sin\alpha = \frac{\rho}{\sqrt{\rho^2 + 4f^2}} \tag{33}$$

$$\cos\alpha = \frac{2f}{\sqrt{\rho^2 + 4f^2}} \tag{34}$$

$$\tan\gamma = \frac{\eta}{\xi} \tag{35}$$

The reflected wave vectors for LL, RR, RL and LR rays are calculated from Fermat's principle of reflection [12], and are given by

$$\mathbf{p}_{LL} = -n_1 \sin 2\alpha \cos\gamma \mathbf{a}_x - n_1 \sin 2\alpha \sin\gamma \mathbf{a}_y - n_1 \cos 2\alpha \mathbf{a}_z \tag{36}$$

$$\mathbf{p}_{RR} = -n_2 \sin 2\alpha \cos\gamma \mathbf{a}_x - n_2 \sin 2\alpha \sin\gamma \mathbf{a}_y - n_2 \cos 2\alpha \mathbf{a}_z \tag{37}$$

$$\mathbf{p}_{RL} = -n_1 S_1 \cos\gamma \mathbf{a}_x - n_1 S_1 \sin\gamma \mathbf{a}_y - n_1 C_1 \mathbf{a}_z \tag{38}$$

$$\mathbf{p}_{LR} = -n_2 S_2 \cos\gamma \mathbf{a}_x - n_2 S_2 \sin\gamma \mathbf{a}_y - n_2 C_2 \mathbf{a}_z \tag{39}$$

where $S_1 = \sin(\alpha + \alpha_1)$, $C_1 = \cos(\alpha + \alpha_1)$, $S_2 = \sin(\alpha + \alpha_2)$ and $C_2 = \cos(\alpha + \alpha_2)$. The initial amplitudes for these rays are given by

$$E_{LL}(r_0) = \frac{\cos\alpha - \cos\alpha_2}{\cos\alpha + \cos\alpha_2} \tag{40}$$

$$E_{RR}(r_0) = \frac{\cos\alpha - \cos\alpha_1}{\cos\alpha + \cos\alpha_1} \tag{41}$$

$$E_{RL}(r_0) = \frac{2\cos\alpha}{\cos\alpha + \cos\alpha_1} \tag{42}$$

$$E_{LR}(r_0) = \frac{2\cos\alpha}{\cos\alpha + \cos\alpha_2} \tag{43}$$

The initial phases are given by

$$s_{LL}(r_o) = n_1\zeta \tag{44}$$

$$s_{RR}(r_0) = n_2\zeta \tag{45}$$

$$s_{RL}(r_0) = n_2\zeta \tag{46}$$

$$s_{LR}(r_0) = n_1\zeta \tag{47}$$

The Jacobian of transformation for these rays are given by

$$J_{LL} = \frac{\cos^4\alpha}{f^2}(n_1 t)^2 - \frac{2\cos^2\alpha}{f} n_1 t + 1 \tag{48}$$

$$J_{RR} = \frac{\cos^4\alpha}{f^2}(n_2 t)^2 - \frac{2\cos^2\alpha}{f} n_2 t + 1 \tag{49}$$

$$\begin{aligned} J_{RL} = & \frac{X_1 S_1 \cos^2\alpha \cot\alpha}{\tan\alpha S_1 + C_1}\left(\frac{n_1^2 t}{2f}\right)^2 \\ & - \frac{S_1^2 - C_1 S_1 \cot\alpha - X_1\cos^2\alpha}{\tan\alpha S_1 + C_1}\left(\frac{n_1 t}{2f}\right) + 1 \end{aligned} \tag{50}$$

$$\begin{aligned} J_{LR} = & \frac{X_2 S_2 \cos^2\alpha \cot\alpha}{\tan\alpha S_2 + C_2}\left(\frac{n_2^2 t}{2f}\right)^2 \\ & - \frac{S_2^2 - C_2 S_2 \cot\alpha - X_2\cos^2\alpha}{\tan\alpha S_2 + C_2}\left(\frac{n_2 t}{2f}\right) + 1 \end{aligned} \tag{51}$$

where

$$X_1 = \frac{\sqrt{n_1^2 - n_2^2 \sin^2 \alpha} + n_2 \cos \alpha}{\sqrt{n_1^2 - n_2^2 \sin^2 \alpha}} \tag{52}$$

$$X_2 = \frac{\sqrt{n_2^2 - n_1^2 \sin^2 \alpha} + n_1 \cos \alpha}{\sqrt{n_2^2 - n_1^2 \sin^2 \alpha}} \tag{53}$$

The focal points equations where Jacobian is zero for LL and RR rays are given as

$$n_1 t = \frac{f}{\cos^2 \alpha} \tag{54}$$

$$n_2 t = \frac{f}{\cos^2 \alpha} \tag{55}$$

Similarly the focal points equations where Jacobian is zero for RL and LR rays are given as

$$\frac{X_1 S_1 \cos^2 \alpha \cot \alpha}{\tan \alpha S_1 + C_1} \left(\frac{n_1^2 t}{2f}\right)^2 - \frac{S_1^2 - C_1 S_1 \cot \alpha - X_1 \cos^2 \alpha}{\tan \alpha S_1 + C_1} \left(\frac{n_1^2 t}{2f}\right) + 1 = 0 \tag{56}$$

$$\frac{X_2 S_2 \cos^2 \alpha \cot \alpha}{\tan \alpha S_2 + C_2} \left(\frac{n_2^2 t}{2f}\right)^2 - \frac{S_2^2 - C_2 S_2 \cot \alpha - X_2 \cos^2 \alpha}{\tan \alpha S_2 + C_2} \left(\frac{n_2^2 t}{2f}\right) + 1 = 0 \tag{57}$$

The geometrical optics field for each ray is obtained by putting Eqs. (40)–(51) in Eq. (18), we get the expression for $u_{LL}(r)$, $u_{RR}(r)$, $u_{RL}(r)$ and $u_{RL}(r)$ as

$$u_{LL}(r) = E_{LL}(r_0) J_{LL}^{-1/2} \exp\left[-jk\left\{n_1^2 t + s_{LL}(r_o)\right\}\right] \tag{58}$$

$$u_{RR}(r) = E_{RR}(r_0) J_{RR}^{-1/2} \exp\left[-jk\left\{n_2^2 t + s_{RR}(r_o)\right\}\right] \tag{59}$$

$$u_{RL}(r) = E_{RL}(r_0) J_{RL}^{-1/2} \exp\left[-jk\left\{n_1^2 t + s_{RL}(r_o)\right\}\right] \tag{60}$$

$$u_{RL}(r) = E_{LR}(r_0) J_{LR}^{-1/2} \exp\left[-jk\left\{n_2^2 t + s_{LR}(r_o)\right\}\right] \tag{61}$$

Since the GO solution fails at the focal points so we find approximate field at focal points using Moslov's method. To calculate the field around the focal points using Eq. (19) we need equation Eq. (20) for the amplitude of different reflected rays

$$J_{LL}(t)\frac{\partial(p_x,p_y)}{\partial(x,y)} = \frac{n_1^2\cos^4\alpha\cos^2 2\alpha}{f^2} \tag{62}$$

$$J_{RR}(t)\frac{\partial(p_x,p_y)}{\partial(x,y)} = \frac{n_2^2\cos^4\alpha\cos^2 2\alpha}{f^2} \tag{63}$$

$$J_{RL}(t)\frac{\partial(p_x,p_y)}{\partial(x,y)} = \frac{X_1 n_1^2 C_1^2 S_1\cos^3\alpha}{4f^2\sin\alpha(\tan\alpha S_1 + C_1)} \tag{64}$$

$$J_{LR}(t)\frac{\partial(p_x,p_y)}{\partial(x,y)} = \frac{X_2 n_2^2 C_2^2 S_2\cos^3\alpha}{4f^2\sin\alpha(\tan\alpha S_2 + C_2)} \tag{65}$$

The amplitude components for each ray is calculated. Now to calculate the phase function in Eq. (19), x and y are expressed in terms of hybrid coordinates (p_x, p_y, z). Similarly t is represented in terms of hybrid coordinates as $t = (z - \zeta)/p_z$. The phase function $s(p_x, p_y)$ is given by

$$s(p_x,p_y) = n\zeta + n^2\left(\frac{z-\zeta}{p_z}\right) - (\xi + p_x t)p_x - (\eta + p_y t)p_y + xp_x + yp_y$$

by putting $\zeta = f\cos 2\alpha/\cos^2\alpha$, $\eta = 2f\tan\alpha\sin\gamma$ and $\xi = 2f\tan\alpha\cos\gamma$ the phase function for different rays are

$$s_{LL}(p_x,p_y) = n_1\left(2f - x\sin 2\alpha\cos\gamma - y\sin 2\alpha\sin\gamma - z\cos 2\alpha\right) \tag{66}$$

$$s_{RR}(p_x,p_y) = n_2\left(2f - x\sin 2\alpha\cos\gamma - y\sin 2\alpha\sin\gamma - z\cos 2\alpha\right) \tag{67}$$

$$\begin{aligned} s_{RL}(p_x,p_y) &= n_1\left\{\frac{n_2}{n_1}f\frac{\cos 2\alpha}{\cos^2\alpha} - (x\cos\gamma + y\sin\gamma - 2f\tan\alpha)S_1\right.\\ &\quad\left. - \left(z - f\frac{\cos 2\alpha}{\cos^2\alpha}\right)C_1\right\} \end{aligned} \tag{68}$$

$$\begin{aligned} s_{LR}(p_x,p_y) &= n_2\left\{\frac{n_1}{n_2}f\frac{\cos 2\alpha}{\cos^2\alpha} - (x\cos\gamma + y\sin\gamma - 2f\tan\alpha)S_2\right.\\ &\quad\left. - \left(z - f\frac{\cos 2\alpha}{\cos^2\alpha}\right)C_2\right\} \end{aligned} \tag{69}$$

The conversion factor from wave vector coordinates (p_x, p_y) in Eq. (19), to ray coordinates (ξ, η) for each ray is given as

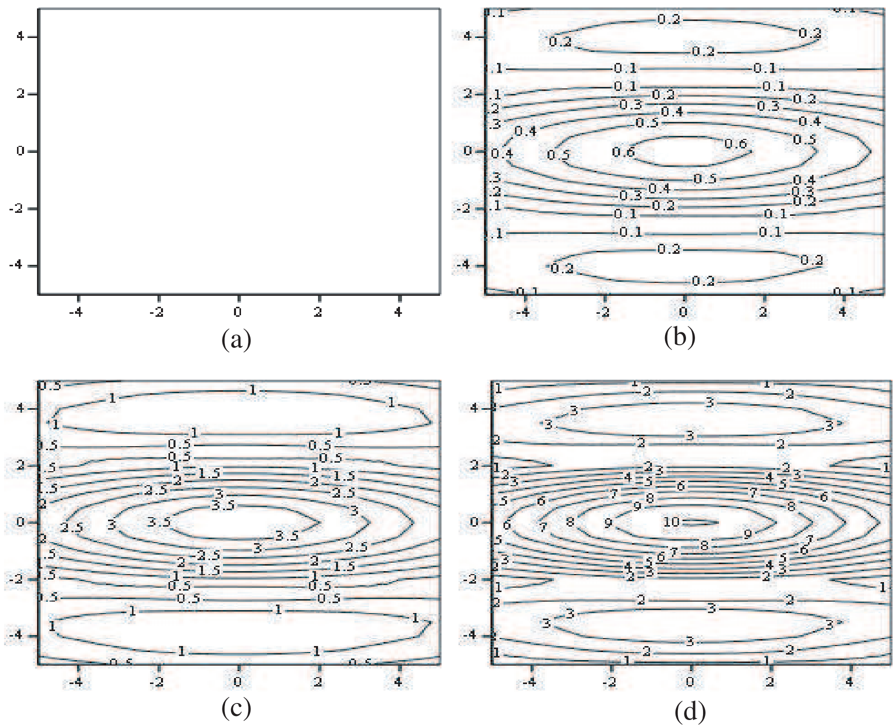

Figure 4. Contour plot for $|u_{LL}|$ with $kf = 100$ and (a) $k\beta = 0$, (b) $k\beta = 0.01$, (c) $k\beta = 0.05$, (d) $k\beta = 0.1$.

$$\frac{\partial(p_{xLL}, p_{yLL})}{\partial(\xi,\eta)} = \frac{n_1^2 \cos^4\alpha \cos 2\alpha}{f^2} \tag{70}$$

$$\frac{\partial(p_{xRR}, p_{yRR})}{\partial(\xi,\eta)} = \frac{n_2^2 \cos^4\alpha \cos 2\alpha}{f^2} \tag{71}$$

$$\frac{\partial(p_{xRL}, p_{yRL})}{\partial(\xi,\eta)} = \frac{n_1^2 X_1 \cos^2\alpha \cot\alpha C_1 S_1}{4f^2} \tag{72}$$

$$\frac{\partial(p_{xLR}, p_{yLR})}{\partial(\xi,\eta)} = \frac{n_2^2 X_2 \cos^2\alpha \cot\alpha C_2 S_2}{4f^2} \tag{73}$$

The conversion factor from (ξ, η) to angular coordinates (α, γ) is given by

$$\frac{\partial(\xi,\eta)}{\partial(\alpha,\gamma)} = \frac{4f^2 \sin\alpha}{\cos^3\alpha} \tag{74}$$

which is the same for LL, RR, RL and LR rays. By substituting

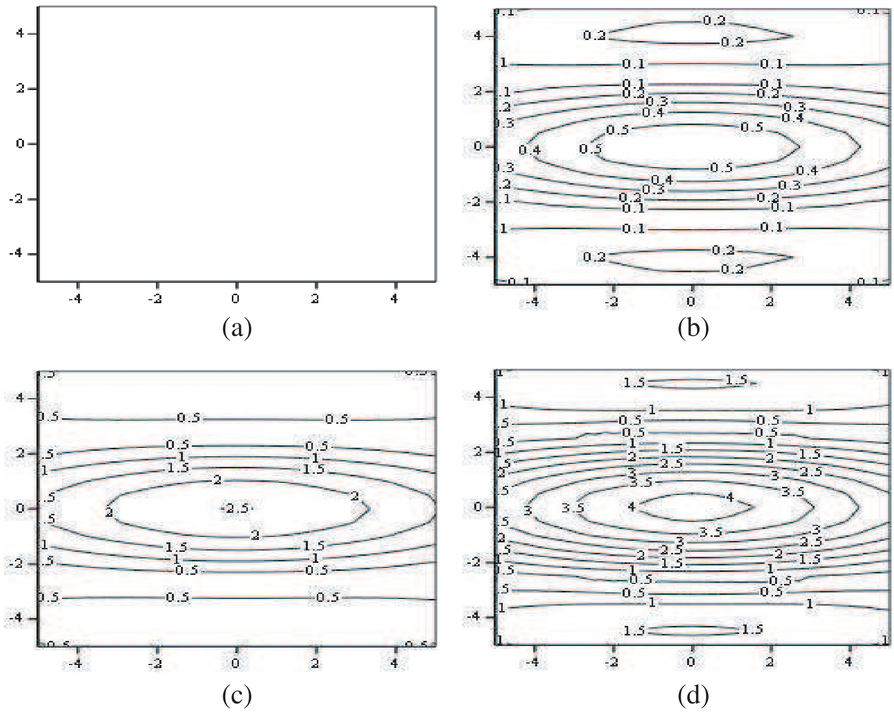

Figure 5. Contour plot for $|u_{RR}|$ with $kf = 100$ and (a) $k\beta = 0$, (b) $k\beta = 0.01$, (c) $k\beta = 0.05$, (d) $k\beta = 0.1$.

Eqs. (62)–(74) in Eq. (19), the field around the focal region of a paraboloidal reflector placed in chiral medium are obtained. The results are given below

$$u_{LL}(r) = \frac{j2kn_1 f}{\pi} \int_0^H \int_0^{2\pi} \left(\frac{\cos\alpha - \cos\alpha_2}{\cos\alpha + \cos\alpha_2} \right) \tan\alpha \times \exp\{-jks_{LL}(p_x, p_y)\} d\alpha d\gamma \tag{75}$$

$$u_{RR}(r) = \frac{j2kn_2 f}{\pi} \int_0^H \int_0^{2\pi} \left(\frac{\cos\alpha - \cos\alpha_1}{\cos\alpha + \cos\alpha_1} \right) \tan\alpha \times \exp\{-jks_{RR}(p_x, p_y)\} d\alpha d\gamma \tag{76}$$

$$u_{RL}(r) = \frac{jkn_1 f}{\pi} \int_0^H \int_0^{2\pi} \left(\frac{2\cos\alpha}{\cos\alpha + \cos\alpha_1} \right) \sec^{3/2}\alpha \sqrt{X_1} \times \{\sin\alpha S_1 (\tan\alpha S_1 + C_1)\}^{1/2} \exp\{-jks_{RL}(p_x, p_y)\} d\alpha d\gamma \tag{77}$$

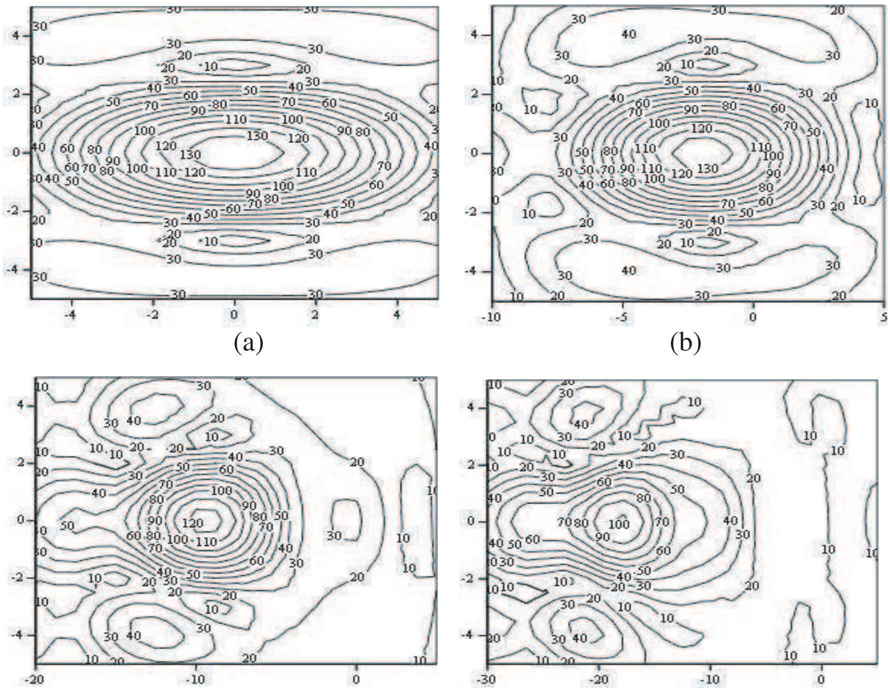

(a) (b) (c) (d)

Figure 6. Contour plot for $|u_{RL}|$ with $kf = 100$ and (a) $k\beta = 0$, (b) $k\beta = 0.01$, (c) $k\beta = 0.05$, (d) $k\beta = 0.1$.

$$u_{LR}(r) = \frac{jkn_2 f}{\pi} \int_0^H \int_0^{2\pi} \left(\frac{2\cos\alpha}{\cos\alpha + \cos\alpha_2} \right) \sec^{3/2}\alpha \sqrt{X_2} \times \{\sin\alpha S_2 (\tan\alpha S_2 + C_2)\}^{1/2} \exp\{-jks_{LR}(p_x, p_y)\} d\alpha d\gamma \quad (78)$$

where $H = \tan^{-1}(D/2f)$, where D is the height of the paraboloidal reflector from the horizontal axis. Eqs. (75)–(78) are solved numerically and the results are presented in the next section.

5. RESULTS AND DISCUSSION

Contour plots of the field reflected by paraboloidal surface placed in isotropic medium are shown in Figures 4–7 and line plots of the paraboloidal reflector are shown in Figures 8–15. For simulation $kf = 100$ and $H = \pi/4$ are used. The fields patterns variation along x-axis, y-axis and z-axis are shown. As the paraboloidal reflector is

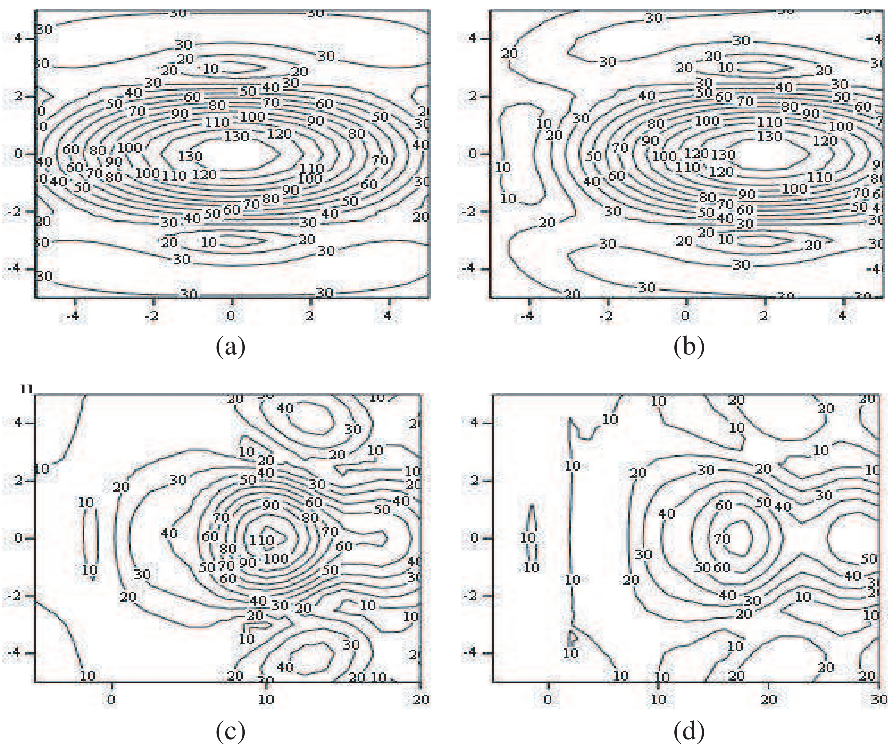

Figure 7. Contour plot for $|u_{LR}|$ with $kf = 100$ and (a) $k\beta = 0$, (b) $k\beta = 0.01$, (c) $k\beta = 0.05$, (d) $k\beta = 0.1$.

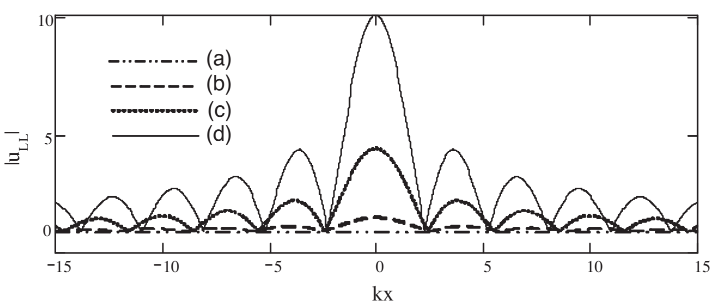

Figure 8. Line plot for $|u_{LL}|$ along either x-axis or y-axis, with $kf = 100$ and (a) $k\beta = 0$, (b) $k\beta = 0.01$, (c) $k\beta = 0.05$, (d) $k\beta = 0.1$.

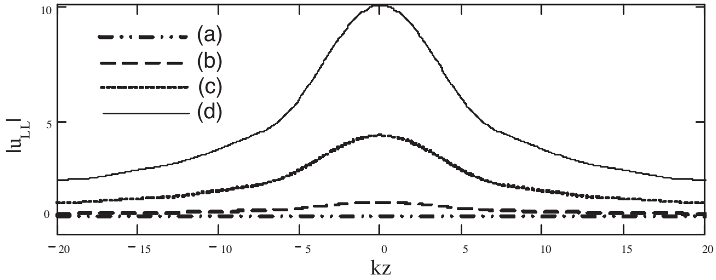

Figure 9. Line plot for $|u_{LL}|$ along z-axis, with $kf = 100$ and (a) $k\beta = 0$, (b) $k\beta = 0.01$, (c) $k\beta = 0.05$, (d) $k\beta = 0.1$.

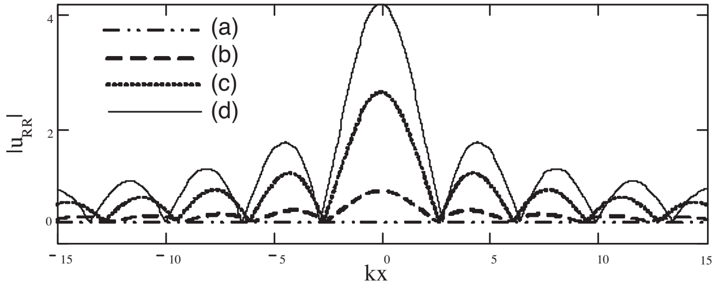

Figure 10. Line plot for $|u_{RR}|$ along either x-axis or y-axis, with $kf = 100$ and (a) $k\beta = 0$, (b) $k\beta = 0.01$, (c) $k\beta = 0.05$, (d) $k\beta = 0.1$.

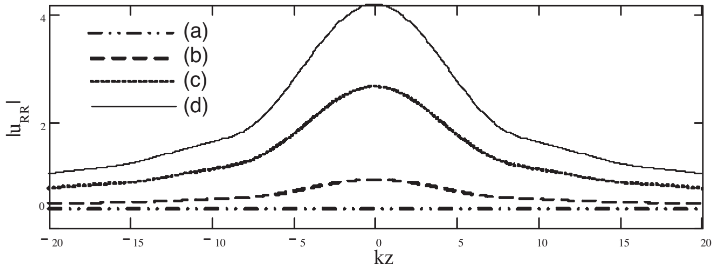

Figure 11. Line plot for $|u_{RR}|$ along z-axis, with $kf = 100$ and (a) $k\beta = 0$, (b) $k\beta = 0.01$, (c) $k\beta = 0.05$, (d) $k\beta = 0.1$.

symmetric, so the magnitude of the field variation along x-axis and y-axis are same. In contour plot horizontal axis is kz and vertical axis is either kx or ky. The solutions of Eqs. (11)–(13), (54), and (55) gives

$$n_1 t = n_2 t = \sqrt{(x-\xi)^2 + (y-\eta)^2 + (z-\zeta)^2} \tag{79}$$

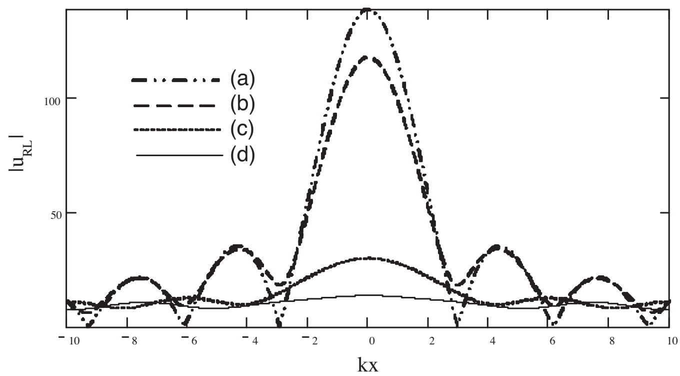

Figure 12. Line plot for $|u_{RL}|$ along either x-axis or y-axis, with $kf = 100$ and (a) $k\beta = 0$, (b) $k\beta = 0.01$, (c) $k\beta = 0.05$, (d) $k\beta = 0.1$.

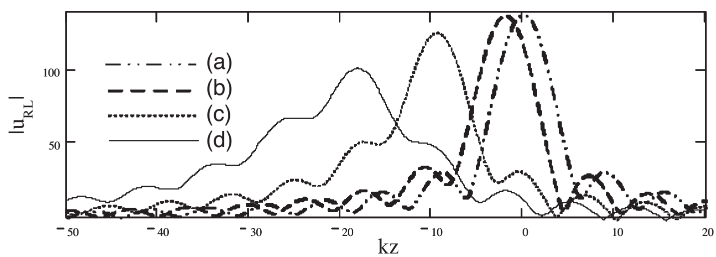

Figure 13. Line plot for $|u_{RL}|$ along z-axis, with $kf = 100$ and (a) $k\beta = 0$, (b) $k\beta = 0.01$, (c) $k\beta = 0.05$, (d) $k\beta = 0.1$.

So the equations of focal points for u_{LL} and u_{RR} of paraboloidal reflector are similar to ordinary medium and overlap which is given by

$$x = y = z = 0 \tag{80}$$

The focal points for LL and RR rays overlap for all values of $k\beta$. For $k\beta = 0$, $n_1 = n_2 = 1$ and

$$u_{LL} = u_{RR} = 0 \tag{81}$$

Magnitude of u_{LL} and u_{RR} around the focal point increases with the increase in the chirality parameter $k\beta$ as shown in Figures 4, 5, 8–11. Magnitude of u_{RL} and u_{LR} around the focal region decrease with the increase of chirality parameter $k\beta$ as shown in Figures 6, 7, 12–15. Figures 6, 7, 13, and 15, show that as the chirality parameter $k\beta$ increases, the focal point for RL is shifted towards left and focal point for LR ray is shifted towards right. With the increase in value of chirality parameter $k\beta$, the gap between the focal points of RL and LR rays increases. The variation in field pattern for different value of the chirality parameter $k\beta$ is shown. If $k\beta = 0$ then $n_1 = n_2 = 1$ and the field pattern reduces to ordinary medium as given in [6]

$$u_{RL} = u_{LR} = \frac{2jkf}{\pi} \int_0^H \int_0^{2\pi} \tan\alpha \exp\{-jk(2f - x\sin 2\alpha\cos\gamma - y\sin 2\alpha\sin\gamma - z\cos 2\alpha)\} d\alpha d\gamma \tag{82}$$

The equation of the focal point for RL and LR rays reduces to Eq. (80), which is the same as in the case of ordinary medium that is achiral medium.

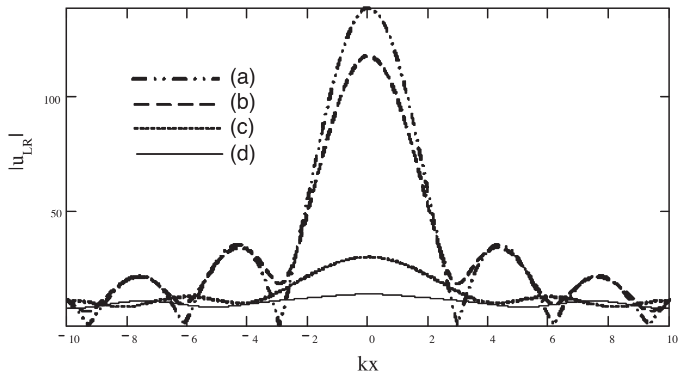

Figure 14. Line plot for $|u_{LR}|$ along either x-axis or y-axis, with $kf = 100$ and (a) $k\beta = 0$, (b) $k\beta = 0.01$, (c) $k\beta = 0.05$, (d) $k\beta = 0.1$.

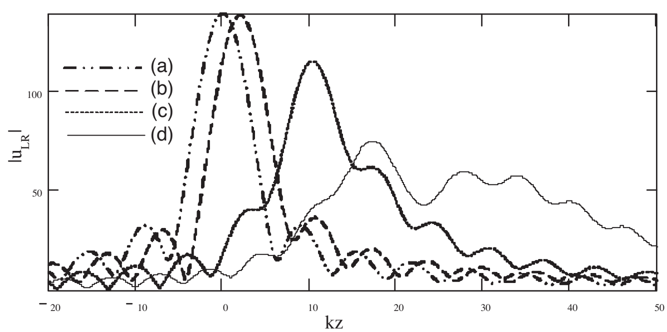

Figure 15. Line plot for $|u_{LR}|$ along z-axis, with $kf = 100$ and (a) $k\beta = 0$, (b) $k\beta = 0.01$, (c) $k\beta = 0.05$, (d) $k\beta = 0.1$.

6. CONCLUSIONS

When a paraboloidal reflector placed in homogenous, isotropic and reciprocal chiral medium is excited, four focal points are formed for different rays designated in this paper by LL, RR, RL and LR. Focal points for LL and RR rays are located at the same position, and focal points for RL and LR are located on the opposite side of the focal point for RR and LL ray. If chirality factor $k\beta > 0$, then LCP wave move slower than RCP, and is focused near the reflector and RCP wave is focused away from the reflector. The situation is reversed if chirality factor $k\beta < 0$. As the chirality parameter increases, the gap between the focal point increases, and if the chirality parameter $k\beta = 0$ is zero, the field for LL and RR becomes zero and that for RL and LR reduces to the case of ordinary medium.

REFERENCES

1. Felson, L. B., *Hybrid Formulation of Wave Propagation and Scattering, Nato ASI Series*, Martinus Nijhoff, Dordrecht, The Netherlands, 1984.
2. Dechamps, G. A., "Ray techniques in electromagnetics," *Proc. IEEE*, Vol. 60, 1022–1035, 1972.
3. Chapman, C. H. and R. Drummond, "Body wave seismograms in inhomogeneous media using Maslov asymptotic theory," *Bull. Seismol., Soc. Am.*, Vol. 72, 277–317, 1982.
4. Maslov, V. P., "Perturbation theory and asymptotic methods," Moskov. Gos. Univ., Moscow, 1965 (in Russian). Translated into Japanese by Ouchi et al., Iwanami.
5. Maslov, V. P. and V. E. Nazaikinski, "Asymptotic of operator and pseudo-differential equations," *Consultants Bureau*, N.Y., 1988.
6. Ghaffar, A., Q. A. Naqvi, and K. Hongo, "Analysis of the fields in three dimensional Cassegrain system," *Progress In Electromagnetics Research*, PIER 72, 215–240, 2007.
7. Hussain, A., Q. A. Naqvi, and K. Hongo, "Radiation characteristics of the Wood lens using Maslov's method," *Progress In Electromagnetics Research*, PIER 73, 107–129, 2007.
8. Ji, Y. and K. Hongo, "Analysis of electromagnetic waves refracted by a spherical dielectric interface by Maslov's method," *J. Opt. Soc. Am. A*, Vol. 8, 541–548, 1991.
9. Ji, Y. and K. Hongo, "Field in the focal region of a dielectric spherical by Maslov's method," *J. Opt. Soc. Am. A*, Vol. 8, 1721–1728, 1991.

10. Hongo, K., Y. Ji, and E. Nakajima, "High frequency expression for the field in the caustic region of a reflector using Maslov's method," *Radio Sci.*, Vol. 21, No. 6, 911–919, 1986.
11. Hongo, K. and Y. Ji, "High frequency expression for the field in the caustic region of a cylindrical reflector using Maslov's method," *Radio Sci.*, Vol. 22, No. 3, 357–366, 1987.
12. Hongo, K. and Y. Ji, "Study of the field around the focal region of spherical reflector antenna by Maslov's method," *IEEE Trans. Antennas Propagat.*, Vol. 36, 592–598, May 1988.
13. Ziolkowski, R. W. and G. A. Deschamps, "Asymptotic evaluation of high frequency field near a caustic: An introduction to Maslov's method," *Radio Sci.*, Vol. 19, 1001–1025, 1984.
14. Faryad, M. and Q. A. Naqvi, "High frequency expression for the field in the caustic region of cylindrical reflector placed in chiral medium," *Progress In Electromagnetics Research*, PIER 76, 153–182, 2007.
15. Faryad, M. and Q. A Naqvi, "High frequency expression for the field in the caustic region of a parabolic reflector coated with isotropic chiral medium," *Journal of Electromagnetic Waves and Applications*, Vol. 22, No. 965–986, 2008.
16. Faryad, M. and Q. A Naqvi, "cylindrical reflector in chiral medium supporting simultaneously positive phase velocity and negative phase velocity," *Journal of Electromagnetic Waves and Applications*, Vol. 22, No. 563–572, 2008.
17. Ghaffar, A., A. Hussain, Q. A. Naqvi, and K. Hongo, "Radiation characteristics of an inhomogeneous slab using Maslov's method," *Journal of Electromagnetic Waves and Applications*, Vol. 22, No. 2, 301–312, 2008.
18. Aziz, A., A. Ghaffar, Q. A. Naqvi, and K. Hongo, "Analysis of the fields in two dimensional Gregorian system," *Journal of Electromagnetic Waves and Applications*, Vol. 22, No. 1, 85–97, 2008.
19. Aziz, A., Q. A. Naqvi, and K. Hongo, "Analysis of the fields in two dimensional Cassegrain system," *Progress In Electromagnetics Research*, PIER 71, 227–241, 2007.
20. Ghaffar, A., A. Rizvi, and Q. A. Naqvi, "Field in the focal space of symmetrical hyperboloidal focusing lens," *Progress In Electromagnetics Research*, PIER 89, 255–273, 2009.
21. Balanis, C. A., *Advanced Engineering Electomagnetics*, John Wiley and Sons, 1989.
22. Lakhtakia, A., "Beltrami fields in chiral media," *Contemporary*

Chemical Physics, World Scientific Series, 1994.

23. Lakhtakia, A., V. K. Varadan, and V. V. Varadan, *Time Harmonic Electromagnetic Fields in Chiral Media*, Springer, Berlin, 1989.
24. Jaggard, D. L., X. Sun, and N. Engheta, "Canonical sources and duality in chiral media," *IEEE Trans. Antennas Propagt.*, Vol. 36, 1007–1013, 1988.
25. Jaggard, D. L., A. R. Mickelson, and C. H. Papas, "On electromagnetic waves in chiral media," *Appl. Phys.*, Vol. 18, 211–216, 1978.
26. Engheta, N. and D. L. Jaggard, "Electromagnetic chirality and its applications," *IEEE Antennas Propagat. Soc. Newsletter*, Vol. 30, 612, 1988.
27. Lakhtakia, A., V. K. Varadan, and V. V. Varadan, "Field equations, huygenss principle, integral equations, and theorems for radiation and scattering of electro-magnetic waves in isotropic chiral media," *J. Opt. Soc. Am. A*, Vol. 5, 175184, 1988.
28. Bassiri, S., "Electromagnetic waves in chiral media," *In Recent Advances in Electromagnetic Theory*, H. N. Kritikos and D. L. Jaggard (eds.), Springer-Verlag, New York, 1990.
29. Engheta, N., "Special issue on wave interaction with chiral and complex media," *Journal of Electromagnetic Waves and Applications*, Vol. 5/6, 537–793, 1992.
30. Lindell, I. V., A. H. Sihvola, S. A. Tretyakov, and A. J. Viitanen, *Electromagnetic Waves in Chiral and Bi-Isotropic Media*, Artech House, MA, 1994.